J. Chem. Eng. Data **2010,** *55,* 3749–3754

Liquid−Liquid Equilibria of Ionic Liquid 1-Butyl-3-Methylimidazolium Tetrafluoroborate + Sodium and Ammonium Citrate Aqueous Two-Phase Systems at (298.15, 308.15, and 323.15) K

Juan Han,[†] Ru Pan,[‡] Xueqiao Xie,[†] Yun Wang,[†] Yongsheng Yan,*[,†] Guowu Yin,[§] and Weixing Guan[||]

School of Chemistry and Chemical Engineering, Jiangsu University, Zhenjiang, China, School of Pharmacy, Jiangsu University, Zhenjiang, China, Tangdu Hospital, The Fourth Military Medical University, Xi'an, China, and School of Environmental Science and Engineering, Chang'an University, Xi'an, China

Binodal curves of the aqueous 1-butyl-3-methylimidazolium tetrafluoroborate ([Bmim]BF_4) + sodium citrate ($Na_3C_6H_5O_7$) and [Bmim]BF_4 + ammonium tartrate ($(NH_4)_3C_6H_5O_7$) systems have been determined experimentally at T = (298.15, 308.15, and 323.15) K. The Merchuk equation was used to correlate the binodal data. The effective excluded volume (EEV) values obtained from the binodal model for these two systems were determined. The binodal curves and EEV both indicate that the salting-out abilities of the two salts follow the order: $Na_3C_6H_5O_7 > (NH_4)_3C_6H_5O_7$. It was demonstrated that the two-phase area was expanded with a decrease in temperature, while the slope of the tie lines slightly decreases with an increase in temperature. The liquid−liquid equilibrium (LLE) data were obtained by density determination and binodal curves correlation of these systems. The Othmer−Tobias and Bancroft and two-parameter equations were used for the correlation of the tie-line data. Good agreement was obtained with the experimental tie-line data with both models.

Introduction

Aqueous two-phase systems (ATPSs) are formed when two components in a water-based solution, which are mutually incompatible, separate into phases of different density under the force of gravity.[1,2] Examples of this phenomenon usually involve either two polymers (e.g., poly(ethylene glycol), PEG, and dextran) or a single polymer plus a high concentration of the appropriate salt.[3,4] In these systems, two or more distinct aqueous phases are formed with a well-defined interface separating them. ATPSs have been used in a wide array of applications, ranging from separation, concentration, and purification of proteins and other biomaterials[5,6] to selective distribution and separation of metallic ions,[7] drug molecules,[8] small organic species,[9] and recovery of nanoparticles.[10]

Recently, more ATPSs[11−13] based on ionic liquids (ILs) have been investigated since Rogers and his co-workers[14] demonstrated that the addition of potassium phosphate to an aqueous solution of a hydrophilic IL produces ATPS. ILs have some "green" characteristics such as negligible volatility and nonflammability under ambient conditions, large liquid range, high thermal and chemical stability, strong solubility power, and a number of possible variations in cation and anion features which allows fine-tuning the IL properties.[15] These new ATPSs have been successfully used to separate drugs,[16,17] proteins,[18] and antibiotics.[19−21]

The most common inorganic salts employed by different research groups on the IL-based aqueous two-phase extraction technique consist of selective cations (ammonium, potassium, or sodium) and anions (phosphate, sulfate, hydroxide, or carbonate). These salts, however, lead to high salt concentrations in effluent streams and, therefore, to environmental concern. In this respect, as an alternative approach Verna and Kula[22] have investigated citrates as a substitute for inorganic salts. Citrates are biodegradable and nontoxic and could be discharged into biological wastewater treatment plants. For analogical reasons, we decided here to examine citrate as an alternative to inorganic salts in IL-based ATPSs.

Phase diagrams and liquid−liquid equilibrium (LLE) data at different temperatures and compositions are essential for the development, optimization, and scale-up of extraction process using ATPS. In this work, we study the phase behavior of the 1-butyl-3-methylimidazolium tetrafluoroborate ([Bmim]BF_4) + sodium citrate ($Na_3C_6H_5O_7$) and [Bmim]BF_4 + ammonium citrate ($(NH_4)_3C_6H_5O_7$) ATPSs at T = (298.15, 308.15, and 323.15) K that have not been previously published. Suitable equations were used to correlate the binodal curve and the tie-line data for the investigated systems. These data provide a possible basis for the prediction of phase composition when such data are not available. In addition, the effective excluded volume (EEV) values obtained from the binodal model for these two systems were determined. The effect of temperature on binodal curves and tie lines of the investigated systems were also discussed.

Experimental Section

Material. [Bmim]BF_4 was purchased from Chenjie Chemical Co., Ltd. (Shanghai, China) with a quoted purity of greater than 0.99 mass fraction and was used without further purification. $Na_3C_6H_5O_7\cdot 2H_2O$ and $(NH_4)_3C_6H_5O_7$ were analytical grade reagents (GR, min. 99 % by mass fraction), which were obtained from Sinopharm Chemical Reagent Co., Ltd. (Shanghai, China).

---

* Corresponding author. Tel.: +86 0511 88790683. Fax: +86 0511 88791800. E-mail address: yys@ujs.edu.cn.

[†] School of Chemistry and Chemical Engineering, Jiangsu University.

[‡] School of Pharmacy, Jiangsu University.

[§] The Fourth Military Medical University.

[||] Chang'an University.

10.1021/je1002797 © 2010 American Chemical Society
Published on Web 07/14/2010

Table 1. Values of Parameters of Equations 1 and 2 for $[Bmim]BF_4$ (1) + $Na_3C_6H_5O_7/(NH_4)_3C_6H_5O_7$ (2) + Water (3) ATPSs at Different Temperatures

T/K	a_1	a_2	a_3	$b_1 \times 10$	$b_2 \times 10^3$	b_3
$[Bmim]BF_4 + Na_3C_6H_5O_7 + H_2O$						
298.15	−2.2767	0.9636	−1.0615	6.3382	−1.9737	−3.3093
308.15	−4.4123	1.6357	−1.0681	5.7706	−3.7862	−4.0024
323.15	−3.0283	1.1763	−1.0721	5.6217	−5.3114	−4.3611
$[Bmim]BF_4 + (NH_4)_3C_6H_5O_7 + H_2O$						
298.15	−3.2160	1.3860	−1.0576	10.4681	−3.6538	−3.4207
308.15	−3.8550	1.6255	−1.0580	9.7949	−5.8504	−3.9232
323.15	−3.9961	1.6592	−1.0623	10.9480	−4.7051	−3.6934

Table 2. Binodal Data for the $[Bmim]BF_4$ (1) + $Na_3C_6H_5O_7$ (2) + H_2O (3) ATPS at T = (298.15, 308.15, and 323.15) K

T = 298.15 K		T = 308.15 K		T = 323.15 K	
100 w_1	100 w_2	100 w_1	100 w_2	100 w_1	100 w_2
79.20	0.26	78.84	0.50	64.31	1.29
70.65	0.44	65.90	0.69	60.47	1.48
66.21	0.49	63.25	0.78	58.33	1.80
62.98	0.69	59.71	0.98	53.69	2.11
59.61	0.80	56.11	1.12	48.16	2.63
52.30	1.26	54.99	1.33	47.48	2.60
47.92	1.51	51.22	1.59	45.79	2.87
44.94	1.85	47.93	1.87	45.10	3.05
40.08	2.20	43.89	2.29	43.58	3.38
37.60	2.40	39.42	2.85	41.73	3.67
34.18	2.66	35.68	3.37	39.25	4.16
31.72	2.94	31.47	3.96	37.91	4.27
28.00	3.49	28.21	4.53	31.36	5.55
25.88	3.77	24.55	5.29	30.42	5.91
22.94	4.52	21.77	6.22	28.84	6.34
20.94	5.08	18.90	7.10	26.89	6.61
17.45	6.61	15.37	9.22	22.66	8.23
15.57	7.43	13.76	10.13	20.80	8.56
14.05	8.57	9.43	14.54	18.82	9.50
12.77	9.63	8.23	16.29	14.46	11.91
10.69	12.28	7.85	16.71	13.82	12.40
8.65	14.09	6.68	19.05	12.15	13.64
7.12	16.74			11.67	14.49
6.77	17.42			9.00	17.39
6.47	18.05			7.59	19.48
5.6	20.07			6.07	22.32

All other reagents were of analytical grade, and double-distilled deionized water was used in the experiments.

Apparatus and Procedure. The binodal curves were determined by the titration method.[3] A glass vessel, volume 50 cm^3, was used to carry out the phase equilibrium determinations. The glass vessel was provided with an external jacket in which water at constant temperature was circulated using a DC-2008 water thermostat (Shanghai Hengping Instrument Factory, China). The temperature was controlled to within ± 0.05 K. An $[Bmim]BF_4$ solution of known mass fraction was taken into the vessel, then a salt solution of known mass fraction was added dropwise to the vessel until the mixture became turbid or cloudy. The composition of this mixture was noted. Afterward, water was added dropwise to the vessel to get a clear one-phase system, and the procedure was repeated and so on. The composition of the mixture for each point on the binodal curve was calculated by mass using an analytical balance (model BS 124S, Beijing Sartorius Instrument Co., China) with a precision of $\pm 1.0 \cdot 10^{-7}$ kg. The maximum uncertainty was found to be 0.001 in determining the mass fraction of both $[Bmim]BF_4$ and salt by titration method used.

Tie-lines were determined from a series of ATPSs by mixing appropriate amounts of $[Bmim]BF_4$, salt, and water in the vessel, which was placed in a thermostatted bath. The system was vigorously stirred for at least 1 h, and the phase separation occurred quickly after cessation of the stirring process. However, a complete phase separation was ensured by centrifuging (model 80-2, Shanghai Surgery Instrument Factory, China) at 2000 rpm for 10 min. Then the systems were placed again into the thermostatted bath and allowed to settle for at least 2 h to separate into two clear phases. After reaching phase equilibrium, the concentration (mass fraction) of salt in the top and bottom phases was determined by density index measurement performed at 298.15 K using a density meter (DMA-4100, Anton Paar Co., Ltd., Austria). The uncertainty in the measurement of the density index was found to be $\pm 0.0001\ g \cdot cm^{-3}$. The relation between the density index d^t, d^b, and the mass fraction of salt, w_2^t, w_2^b, in top and bottom phases was given by

$$d^t = a_1 - a_2 \ln(a_3 w_2^t) \tag{1}$$

$$d^b = b_1 + b_2 \exp(b_3 w_2^b) \tag{2}$$

where a_1, a_2, a_3, b_1, b_2, and b_3 are constants for the same salt. The density data, ρ, and the mass fraction of salt, w_2^t, w_2^b, in top and bottom phases were given in the Tables S1 and S2 of Supporting Information. The values of coefficients a_1, a_2, a_3, b_1, b_2, and b_3 for the applied systems are given in Table 1. Using eqs 1 and 2, the precision of the mass fraction of salt better than 0.001 has been achieved. The mass fraction of $[Bmim]BF_4$ in both phases was calculated by the correlation of the Merchuk equation. The mass fraction of water was then calculated.

The tie-line length, TLL, and the slope of the tie-line, S, at different compositions were also calculated, respectively, using eqs 3 and 4 as follows

$$\mathrm{TLL} = [(w_1^t - w_1^b)^2 + (w_2^t - w_2^b)^2]^{0.5} \tag{3}$$

$$S = (w_1^t - w_1^b)/(w_2^t - w_2^b) \tag{4}$$

where w_1^t, w_1^b, w_2^t, and w_2^b represent the equilibrium mass fraction of $[Bmim]BF_4$ (1) and salt (2), in the top, t, and bottom, b, phases, respectively.

Results and Discussion

Binodal Data and Correlation of Merchuk Equation. The binodal data, for the $[Bmim]BF_4 + Na_3C_6H_5O_7/(NH_4)_3C_6H_5O_7$ + water ATPSs, representing the minimum concentration required for the formation of two phases at temperatures (298.15, 308.15, and 323.15) K are given in Tables 2 and 3. For the studied systems, the experimental binodal data were fitted by a least-squares regression method to the following empirical nonlinear expression developed by Merchuk[23]

$$w_1 = a \exp(b {w_2}^{0.5} - c {w_2}^3) \tag{5}$$

where w_1 and w_2 are the mass fractions of $[Bmim]BF_4$ and salt, respectively. Recently, the above equation has been successfully used for the correlation of binodal data of some aqueous PEG + salt[24,25] and IL + salt[26−28] ATPSs. Using eq 5, the fitting parameters a, b, and c obtained from the correlation of experimental binodal data along with the correlation coefficient (R^2) and the corresponding standard deviations (SD) are given in Table 4. The binodals reproduced from eq 5 at different temperatures are also shown in Figure 1. On the basis of

Table 3. Binodal Data for the [Bmim]BF$_4$ (1) + (NH$_4$)$_3$C$_6$H$_5$O$_7$ (2) + H$_2$O (3) ATPS at T = (298.15, 308.15, and 323.15) K

T = 298.15 K		T = 308.15 K		T = 323.15 K	
100 w_1	100 w_2	100 w_1	100 w_2	100 w_1	100 w_2
72.19	0.59	74.96	0.51	67.83	1.26
68.11	0.68	72.37	0.58	57.35	1.94
60.83	0.94	65.63	0.91	53.66	2.44
53.48	1.38	61.49	1.06	44.9	3.63
46.49	1.89	52.33	1.74	38.76	4.76
42.07	2.26	45.17	2.31	34.28	5.61
38.08	2.58	38.18	3.22	28.29	6.89
34.50	2.96	36.83	3.54	24.70	8.04
31.06	3.42	32.76	4.21	22.87	9.21
27.67	4.16	29.63	4.93	21.81	9.34
23.01	5.21	25.52	5.97	20.20	10.45
21.34	5.80	23.40	6.51	18.61	11.30
19.60	6.57	20.99	7.59	16.52	12.72
18.10	7.38	19.61	8.25	14.88	14.35
16.15	8.64	18.01	9.04	13.88	15.31
15.78	8.99	15.72	10.89	12.19	17.42
14.85	9.83	14.16	11.97	10.39	19.64
13.97	10.54	12.61	13.68	9.74	20.26
12.11	12.47	11.15	15.96	8.50	22.54
11.17	13.59	9.93	17.95	7.97	24.06
10.74	14.34	8.44	20.08	7.46	24.69
9.52	16.27	7.31	22.62	7.13	25.96
9.27	17.31	6.56	24.38		
8.77	18.39	5.78	27.75		
8.00	19.18				
7.84	20.17				
7.25	21.93				
6.94	22.32				
6.41	23.11				
5.82	25.75				

Table 4. Values of Parameters of Equation 5 for the [Bmim]BF$_4$ (1) + Na$_3$C$_6$H$_5$O$_7$/(NH$_4$)$_3$C$_6$H$_5$O$_7$ (2) + H$_2$O (3) ATPSs at T = (298.15, 308.15, and 323.15) K

T/K	a	b	$c \cdot 10^{-5}$	R^2	100 SD[a]
		[Bmim]BF$_4$ + Na$_3$C$_6$H$_5$O$_7$ + H$_2$O			
298.15	115.05397	−0.73421	−4.36807	0.99721	1.11
308.15	112.83765	−0.64206	1.30192	0.99819	0.84
323.15	126.73959	−0.59235	3.78356	0.99775	0.79
		[Bmim]BF$_4$ + (NH$_4$)$_3$C$_6$H$_5$O$_7$ + H$_2$O			
298.15	122.18516	−0.71131	−4.77197	0.99728	0.96
308.15	116.87849	−0.61988	−1.53418	0.99955	0.43
323.15	129.42691	−0.57053	0.08402	0.99854	0.63

[a] SD = $(\sum_{i=1}^{n}(w_1^{\mathrm{cal}} - w_1^{\mathrm{exp}})^2/n)^{0.5}$, where w_1 and n represent the concentration (in mass percent) of [Bmim]BF$_4$ and the number of binodal data, respectively.

obtained SDs, eq 5 can be satisfactorily used to correlate the binodal curves of the investigated systems.

Effect of Temperature on Binodal Curves. The effect of temperature on the phase-forming ability for the studied systems is also illustrated in Figure 1. The locus for the experimental binodals demonstrates that the two-phase area is expanded with a decrease in temperature, which is attributed to the decrease in solubility of IL or the increase in the phase-forming ability in the studied system. This is because the effect of a decrease in temperature on the structure of water is qualitatively similar to that of a kosmotropic (structure-making) ion and therefore can promote the phase-forming ability in the investigated system as a favorable factor for salting-out of IL. More recently, the effect of temperature on the phase-forming ability in the [Bmim]BF$_4$ + Na$_2$CO$_3$/NaH$_2$PO$_4$ two-phase system[29] and [C$_4$mim]Br + tripotassium citrate two-phase system[30] has also demonstrated that the two-phase area is expanded with a decrease in temperature. A possible reason is that the hydration sheath around the [Bmim]BF$_4$ in aqueous [Bmim]BF$_4$ + Na$_3$C$_6$H$_5$O$_7$/(NH$_4$)$_3$C$_6$H$_5$O$_7$ ATPS is more sensitive to temperature because of a decreased kosmotropicity of the citrate ion.

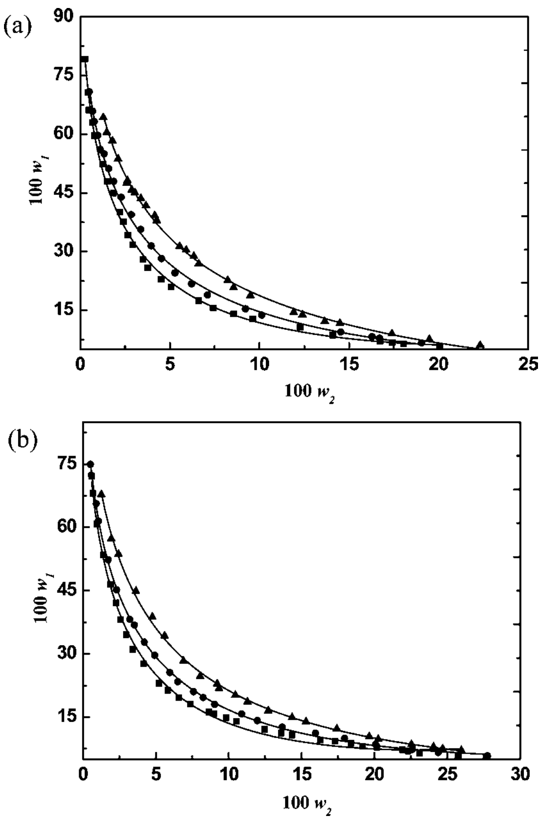

Figure 1. Effect of temperature on binodal curves of the [Bmim]BF$_4$ (1) + Na$_3$C$_6$H$_5$O$_7$/(NH$_4$)$_3$C$_6$H$_5$O$_7$ (2) + H$_2$O (3) ATPS: (a) Na$_3$C$_6$H$_5$O$_7$; (b) (NH$_4$)$_3$C$_6$H$_5$O$_7$; ■, 298.15 K; ●, 308.15 K; ▲, 323.15 K.

EEV and Salting-out Ability of Salts. The binodal model which based on the statistical geometry methods is developed by Guan et al.[31] for aqueous polymer−polymer systems. In the present work, our team used this model to calculate the EEV of salt in different hydrophilic alcohol−water component solvents.[32] In this paper, the binodal equation for the aqueous ionic liquid−salt systems can be written as

$$\ln\left(V_{213}^{*}\frac{w_2}{M_2} + f_{213}\right) + V_{213}^{*}\frac{w_1}{M_1} = 0 \tag{6}$$

$$\ln\left(V_{213}^{*}\frac{w_2}{M_2}\right) + V_{213}^{*}\frac{w_1}{M_1} = 0 \tag{7}$$

where V_{213}^{*}, f_{213}, M_1, and M_2 are the scaled EEV of salt, the volume fraction of unfilled effective available volume after tight packing of salt molecules into the network of ionic liquid molecules in ionic liquid aqueous solutions, which includes the influence of the size of the water molecules and the molar mass of ionic liquid and salt, respectively.

In the original application, eq 7 was used to correlate binodal data of polymer−polymer systems because of the marked difference in size between the two components. The f_{213} value will be very small and consequently can be neglected. The EEV represents the smallest spacing of an individual ionic liquid which will accepted an individual salt, so it reflects the compatibility of components in the same system. For the investigated systems, the EEV and f_{213} values obtained from the correlation of the experimental binodal along with the

Table 5. Values of Parameters of EEV of Salts Using Equation 6 or 7 for the [Bmim]BF_4 (1) + $Na_3C_6H_5O_7$/$(NH_4)_3C_6H_5O_7$ (2) + H_2O (3) ATPSs at *T* = (298.15, 308.15, and 323.15) K

salt	*T*/K	$V^*_{213} \cdot 10^3$ (g·mol^{-1})	$f_{213} \cdot 10^{-3}$	R^2	100 SD[a]
$Na_3C_6H_5O_7$	298.15	1.26280		0.98401	3.18
	308.15	1.11846		0.99210	1.98
	323.15	1.04754		0.99416	1.52
$(NH_4)_3C_6H_5O_7$	298.15	1.15347	0.10	0.94227	4.85
	308.15	1.06011	8.86	0.96743	4.06
	323.15	0.89709	28.90	0.96397	3.44

[a] SD = $(\sum_{i=1}^{n}(w_1^{\mathrm{cal}} - w_1^{\mathrm{exp}})^2/n)^{0.5}$, where w_1 and *n* represent the concentration (in mass percent) of [Bmim]BF_4 and the number of binodal data, respectively.

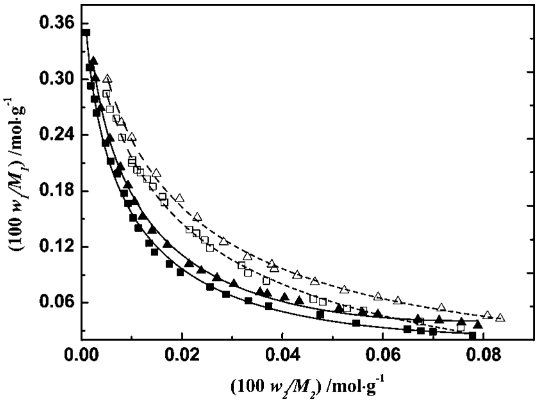

Figure 2. Effect of the type of salts on the binodal curves plotted in molality for the [Bmim]BF_4 (1) + $Na_3C_6H_5O_7$/$(NH_4)_3C_6H_5O_7$ (2) + H_2O (3) ATPSs at (298.15 and 323.15) K. □, $Na_3C_6H_5O_7$; △, $(NH_4)_3C_6H_5O_7$; solid, 298.15 K; hollow, 323.15 K.

corresponding correlation coefficients (R^2) and SDs are given in Table 5. From the table, it was found that the parameter f_{213} was not so small as to be neglected for the [Bmim]BF_4 + $(NH_4)_3C_6H_5O_7$ + water ATPS, and eq 6 showed a much higher accuracy in binodal data fitting than eq 7. Nevertheless, as for the [Bmim]BF_4 + $Na_3C_6H_5O_7$ + water ATPS, there was no significant difference between these two equations in binodal data fitting, so a simplified eq 7 can be used. On the basis of SDs presented in Table 4, the Merchuk equation (eq 5) with three parameters presents satisfactory results in correlation of the experimental binodal data, while the binodal model (eq 6 or 7) with only two or one parameters gives rather poor results. However, the rank order of the EEV values ($Na_3C_6H_5O_7$ > $(NH_4)_3C_6H_5O_7$) at the same temperature indicates that the fitted parameters, V^*_{213}, should, in the investigated systems with a specific ionic liquid, be related to the salting-out strength of salt, similar to aqueous polymer−salt systems.[24,25] To examine more closely the relation between the EEV values and the salting-out strength, the binodals of the investigated systems are plotted in Figure 2 where the concentration of the two components is expressed in molality.

As shown in Figure 2 and Table 5, it was found that the salts with higher salting-out strength have larger values of EEV at the same temperature. The increase of the EEV value is reflected in the phase diagram by a shift in the position of the binodal curve to the left, corresponding to a decrease in the area representing the single-phase mixture; thus, a decrease in the concentration of salt required to form a two-phase system indicates the higher salting-out strength of the salt. Similar to polymer−salt ATPSs, the salting-out ability of salts can also be related to the Gibbs free energy of hydration of the constituent ions (ΔG_{hyd}).[24,33] When comparing salts having the same anion, the one whose cation has a more negative ΔG_{hyd} value is better at salting-out IL. Thus, from Figure 2 it easy to see that the salting-out ability of the cations follows the ordering Na^+ > NH_4^+. This ordering directly follows the cations' ΔG_{hyd} values (Na^+, −365 kJ·mol^{-1} > NH_4^+, −285 kJ·mol^{-1}).[34]

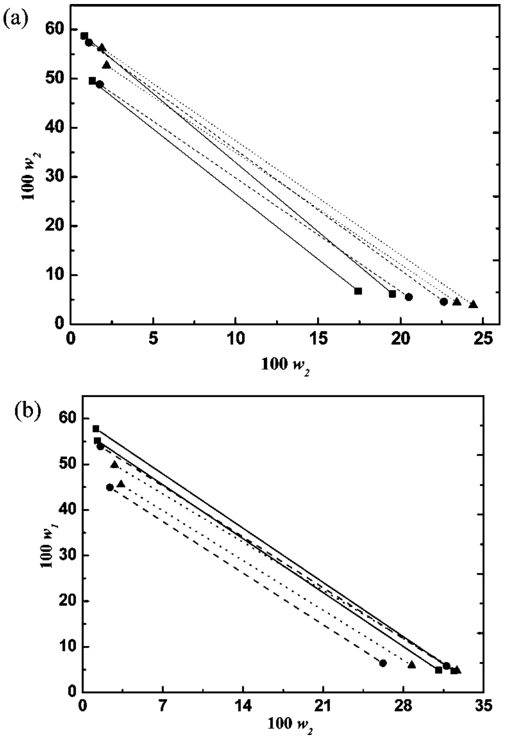

Figure 3. Effect of temperature on the equilibrium phase compositions of the [Bmim]BF_4 (1) + $Na_3C_6H_5O_7$/$(NH_4)_3C_6H_5O_7$ (2) + H_2O (3) ATPS: (a), $Na_3C_6H_5O_7$; (b), $(NH_4)_3C_6H_5O_7$; ■, 298.15 K; ●, 308.15 K; ▲, 323.15 K; —, tie lines at 298.15 K; – –, tie lines at 308.15 K; ···, tie lines at 323.15 K. These tie lines were obtained by connecting the experimental equilibrium phase composition data.

Table 6. Tie-Line Data for the [Bmim]BF_4 (1) + $Na_3C_6H_5O_7$ (2)+ H_2O (3) ATPSs at *T* = (298.15, 308.15, and 323.15) K

	total system		top phase		bottom phase			
T/K	100 w_1	100 w_2	100 w_1	100 w_2	100 w_1	100 w_2	TLL	*S*
298.15	41.97	6.57	58.73	0.84	6.22	19.50	55.73	−2.81
	39.08	5.26	49.54	1.32	6.76	17.44	45.72	−2.65
	37.68	6.13	50.68	1.25	6.84	18.21	47.01	−2.58
	32.02	4.39	37.41	2.34	7.65	15.23	32.43	−2.31
308.15	33.84	12.16	61.36	0.90	4.24	23.49	61.42	−2.53
	30.10	14.97	68.04	0.62	3.93	24.36	68.36	−2.70
	40.20	7.95	57.37	1.11	4.58	22.63	57.01	−2.45
	38.97	6.02	48.84	1.77	5.51	20.50	47.20	−2.31
323.15	37.93	9.01	52.71	2.19	4.45	23.41	52.72	−2.27
	38.98	11.86	64.02	1.33	2.99	26.46	66.00	−2.43
	33.97	11.55	56.24	1.89	3.92	24.40	56.96	2.32
	38.81	13.94	68.87	1.06	2.13	28.81	72.28	−2.41

LLE Data and Effect of Temperature on Tie lines. For the [Bmim]BF_4 + $Na_3C_6H_5O_7$/$(NH_4)_3C_6H_5O_7$ + H_2O ATPSs, the density data of LLE were given in Table S3 and S4 of Supporting Information. According to the density data of LLE, the tie-line compositions at *T* = (298.15, 308.15, and 323.15) K are given in Tables 6 and 7. For most of the systems, the IL concentration in the bottom phase is very small, and in some cases, the IL is almost excluded completely from the phase. The opposition behavior is observed in the top phase.

Additionally, to show the effect of temperature on the equilibrium phase compositions for the investigated system, the experimental tie lines are compared in Figure 3 for the temperatures *T* = (298.15, 308.15, and 323.15) K. As shown

Table 7. Tie-Line Data for the [Bmim]BF$_4$ (1) + (NH$_4$)$_3$C$_6$H$_5$O$_7$ (2) + H$_2$O (3) ATPSs at (298.15, 308.15, and 323.15) K

	total system		top phase		bottom phase			
T/K	100 w_1	100 w_2	100 w_1	100 w_2	100 w_1	100 w_2	TLL	S
298.15	29.99	9.00	41.21	2.32	6.59	23.13	40.39	−1.66
	34.95	12.99	55.13	1.30	4.90	31.08	58.39	−1.69
	30.00	18.98	61.49	0.98	4.48	34.58	66.17	−1.70
	31.95	16.35	57.78	1.16	4.72	32.44	61.59	−1.70
308.15	34.99	15.99	59.95	1.16	5.75	34.09	63.42	−1.65
	30.66	11.03	44.93	2.38	6.44	26.23	45.28	−1.61
	30.01	17.96	57.18	1.33	5.76	33.30	60.55	−1.61
	30.03	16.99	53.89	1.56	5.81	31.77	56.78	−1.60
323.15	29.91	16.49	49.82	2.80	4.82	32.69	54.21	−1.51
	29.91	12.90	45.55	3.35	5.96	28.74	47.03	−1.56
	29.96	17.02	52.51	2.50	4.68	33.23	56.85	−1.56
	30.00	20.53	59.57	1.85	3.77	37.48	66.21	−1.57

Table 8. Values of Parameters of Equations 8 and 9 for the [Bmim]BF$_4$(1) + Na$_3$C$_6$H$_5$O$_7$/(NH$_4$)$_3$C$_6$H$_5$O$_7$ (2) + H$_2$O (3) ATPSs at (298.15, 308.15, and 323.15) K

T/K	k_1	n	R^2	k_2	r	R^2	100 SD$_1$[a]	100 SD$_2$[a]
				[Bmim]BF$_4$ + Na$_3$C$_6$H$_5$O$_7$ + H$_2$O				
298.15	0.0132	2.8215	0.976	4.2946	0.3396	0.970	1.05	1.46
308.15	0.0103	3.4343	0.944	3.5496	0.2618	0.943	1.20	1.61
323.15	0.0465	2.4859	0.983	3.2748	0.3628	0.982	0.70	0.72
				[Bmim]BF$_4$ + (NH$_4$)$_3$C$_6$H$_5$O$_7$ + H$_2$O				
298.15	0.2527	1.4456	0.998	2.4442	0.6790	0.998	0.38	0.34
308.15	0.2535	1.5366	0.970	2.2835	0.6533	0.972	1.04	0.99
323.15	0.3337	1.4395	0.947	2.0556	0.6467	0.948	1.29	1.34

[a] SD = $[\sum_{i=1}^{N}((w_{i,j,\mathrm{cal}}^{\mathrm{top}} - w_{i,j,\mathrm{exp}}^{\mathrm{top}})^2 + (w_{i,j,\mathrm{cal}}^{\mathrm{bot}} - w_{i,j,\mathrm{exp}}^{\mathrm{bot}})^2)/2N]^{0.5}$ where N is the number of tie lines and $j = 1$ and $j = 2$, SD$_1$ and SD$_2$ represent the mass percent standard deviations for [Bmim]BF$_4$ and salt, respectively.

in Figure 3, it was found that the slope of the tie lines slightly decrease with an increase in temperature. This trend means that when the temperature is decreased, water is driven from the [Bmim]BF$_4$-rich phase to the salt-rich phase, so the [Bmim]BF$_4$ concentration at the [Bmim]BF$_4$-rich phase increases, whereas the salt-rich phase will be somewhat more diluted. In other words, water becames a poorer solvent for [Bmim]BF$_4$ as the temperature is decreased.

Correlation of the LLE Data. The correlation equations[35] given by Othmer−Tobias (eq 8) and Bancroft (eq 9) have also been used to correlate the tie-line compositions.

$$\left(\frac{1 - w_1^{\mathrm{t}}}{w_1^{\mathrm{t}}}\right) = k_1\left(\frac{1 - w_2^{\mathrm{b}}}{w_2^{\mathrm{b}}}\right)^n \tag{8}$$

$$\left(\frac{w_3^{\mathrm{b}}}{w_2^{\mathrm{b}}}\right) = k_2\left(\frac{w_3^{\mathrm{t}}}{w_1^{\mathrm{t}}}\right)^r \tag{9}$$

where w_1^{t} is the mass fraction of ILs in the top phase; w_2^{b} is the mass fraction of salt in the bottom phase; w_3^{b} and w_3^{t} are the mass fraction of water in the bottom and top phases, respectively; and k_1, n, k_2, and r are the fit parameters.

Recently, eqs 8 and 9 have been successfully used for the correlation of the tie-line compositions of the imidazolium ionic liquids + salt or sucrose + water ATPSs.[26,27] A linear dependency of the plots log $[(1 - w_1^{\mathrm{t}})/w_1^{\mathrm{t}}]$ against log$[(1 - w_2^{\mathrm{b}})/w_2^{\mathrm{b}}]$ and log$(w_3^{\mathrm{b}}/w_2^{\mathrm{b}})$ against log$(w_3^{\mathrm{t}}/w_1^{\mathrm{t}})$ indicated an acceptable consistency of the results. The values of the parameters k_1, n, k_2, and r of equations with the corresponding correlation coefficient values (R^2) and SDs are given in Table 8, and it is indicated that eqs 8 and 9 can be satisfactorily used to correlate the tie-line data of the investigated systems.

Table 9. Values of Parameters of Equation 10 for the [Bmim]BF$_4$ (1) + Na$_3$C$_6$H$_5$O$_7$/(NH$_4$)$_3$C$_6$H$_5$O$_7$ (2) + H$_2$O (3) ATPSs at (298.15, 308.15, and 323.15) K

T/K	k	β	R^2	100 SD[b]
		[Bmim]BF$_4$ + Na$_3$C$_6$H$_5$O$_7$ + H$_2$O		
298.15	5.5970	−0.2063	0.9987	0.28
308.15	5.8743	0.0926	0.9998	0.09
323.15	5.0423	0.0735	0.9988	0.27
		[Bmim]BF$_4$ + (NH$_4$)$_3$C$_6$H$_5$O$_7$ + H$_2$O		
298.15	5.6273	−0.3499	0.9999	0.11
308.15	6.2754	0.0115	0.9995	0.18
323.15	5.2696	−0.0710	0.9986	0.25

[b] SD = $[\sum_{j=1}^{3}\sum_{i=1}^{N}((w_{i,j,\mathrm{cal}}^{\mathrm{top}} - w_{i,j,\mathrm{exp}}^{\mathrm{top}})^2 - (w_{i,j,\mathrm{cal}}^{\mathrm{bot}} - w_{i,j,\mathrm{exp}}^{\mathrm{bot}})^2)/6N]^{0.5}$ where N is the number of tie-lines and j is the number of components in each phase.

In this work, a relatively simple two-parameter equation was used to correlate the tie-lines data, which can be derived from the binodal theory.[31] The equation used has the following form:

$$\ln\left(\frac{w_2^{\mathrm{t}}}{w_2^{\mathrm{b}}}\right) = \beta + k(w_1^{\mathrm{b}} - w_1^{\mathrm{t}}) \tag{10}$$

In which k is the salting-out coefficient, and β is the constant related to the activity coefficient. Superscripts "t" and "b" stand for the IL-rich phase and salt-rich phase, respectively. Recently, eq 10 was successfully used for the correlation of tie-line data for the polymer-salt ATPSs.[24,36] The fitting parameters of eq 10, along with the corresponding SDs, are presented in Table 9 for the investigated systems. On the basis of the SDs reported in Table 9, eq 10 represents the experimental LLE data with a good accuracy at each temperature.

Conclusion

LLE data for the [Bmim]BF$_4$ + Na$_3$C$_6$H$_5$O$_7$/(NH$_4$)$_3$C$_6$H$_5$O$_7$ + H$_2$O ATPSs were obtained at T = (298.15, 308.15, and

323.15) K. The experimental binodal data were satisfactorily correlated with the Merchuk equation. Using the binodal model, the EEV were calculated for these two systems at different temperatures. It was shown that the EEV values are related to the salting-out strength of salt. The effectiveness of the studied salts to form ATPSs with [Bmim]BF_4 was also discussed on the basis of Gibbs free energy of hydration of salt constituent ions. It was found that, for the studied systems, the cation with a more negative ΔG_{hyd} value is better at salting-out and it also causes the expansion of the two-phase area. The two-phase area was expanded with a decrease in temperature, while the slope of the tie lines was slightly decreased with an increase in temperature. Furthermore, the tie-line data were successfully correlated with the Othmer−Tobias and Bancroft equations, as well as the two-parameter equation.

Supporting Information Available:

Tables S1−S4 contain density data for the ATPSs. This material is available free of charge via the Internet at http://pubs.acs.org.

Literature Cited

(1) Sinha, J.; Dey, P. K.; Panda, T. Aqueous Two-phase: the system of choice for extractive fermentation. *Appl. Microbiol. Biotechnol.* **2000**, *54*, 476–486.

(2) Hatti-Kaul, R. *Aqueous-Phase Systems: Methods and Protocols*; Methods in Biotechnol 11; Humana Press: Totowa, NJ, 2000.

(3) Albertsson, P.-A. *Partitioning of Cell Particles and Macromolecules*; J. Wiley & Sons: New York, 1986.

(4) Baxter, S. M.; Sperry, P. R.; Fu, Z. Partitioning of polymer and inorganic colloids in two-phase aqueous polymer systems. *Langmuir* **1997**, *13*, 3948–3952.

(5) Silva, C. A. S.; Coimbra, J. S. R.; Rojas, E. E. G.; Minim, L. A.; Silva, L. H. M. Partitioning of caseinomacropeptide in aqueous two-phase systems. *J. Chromatogr., B* **2007**, *858*, 205–210.

(6) Rosa, P. A. J.; Azevedo, A. M.; Aires-Barros, M. R. Application of central composite design to the optimization of aqueous two-phase extraction of human antibodies. *J. Chromatogr., A* **2007**, *1141*, 50–60.

(7) Silva, L. H. M.; Silva, M. C. H.; Amim Júnior, J.; Martins, J. P.; Coimbra, J. S. R.; Minim, L. A. Hydrophobic effect on the partitioning of $[Fe(CN)_5(NO)]^{2-}$ and $[Fe(CN)_6]^{3-}$ anions in aqueous two-phase systems formed by triblock copolymers and phosphate salts. *Sep. Purif. Technol.* **2008**, *60*, 103–112.

(8) Agasøster, T. Aqueous two-phase partitioning sample preparation prior to liquid chromatography of hydrophilic drugs in blood. *J. Chromatogr., B* **1998**, *716*, 293–298.

(9) Willauer, H. D.; Huddleston, J. G.; Rogers, R. D. Solute partitioning in aqueous biphasic systems composed of polyethylene glycol and salt: the partitioning of small neutral organic species. *Ind. Eng. Chem. Res.* **2002**, *41*, 1892–1904.

(10) Braas, G. M. F.; Walker, S. G.; Lyddiatt, A. recovery in aqueous two-phase systems of nanoparticulates applied as surrogate mimics for viral gene therapy vectors. *J. Chromatogr., B* **2000**, *743*, 409–419.

(11) Zafarani-Moattar, M. T.; Hamzehzadeh, S. Liquid-liquid equilibria of aqueous two-phase systems containing 1-butyl-3-methylimidazolium bromide and potassium phosphate or dipotassium hydrogen phosphate at 298.15K. *J. Chem. Eng. Data* **2007**, *52*, 1686–1692.

(12) Deng, Y. F.; Chen, J.; Zhang, D. L. Phase diagram data for several salt + salt aqueous biphasic systems at 298.15 K. *J. Chem. Eng. Data* **2007**, *52*, 1332–1335.

(13) Bridges, N. J.; Gutowski, K. E.; Rogers, R. D. Investigation of aqueous biphasic systems formed from solutions of chaotropic salts with kosmotropic salts (salt-salt ABS). *Green Chem.* **2007**, *9*, 177–183.

(14) Gutowski, K. E.; Broker, G. A.; Willauer, H. D.; Huddleston, J. G.; Swatloski, R. P.; Holbrey, J. D.; Rogers, R. D. Controlling the aqueous miscibility of ionic Liquids: aqueous biphasic systems of water-miscible ionic liquids and water-structuring salts for recycle, metathesis, and separations. *J. Am. Chem. Soc.* **2003**, *125*, 6632–6633.

(15) Han, X.; Armstrong, D. W. Ionic liquids in separations. *Acc. Chem. Res.* **2007**, *40*, 1079–1086.

(16) He, C.; Li, S.; Liu, H.; Li, K.; Liu, F. Extraction of testosterone and epitestosterone in human urine using aqueous two-phase systems of ionic liquid and salt. *J. Chromatogr., A* **2005**, *1082*, 143–149.

(17) Li, S.; He, C.; Liu, H.; Li, K.; Liu, F. Ionic liquid-based aqueous two-phase system, a sample pretreatment procedure prior to high-performance liquid chromatography of opium alkaloids. *J. Chromatogr., B* **2005**, *826*, 58–62.

(18) Du, Z.; Yu, Y. L.; Wang, J. H. Extraction of proteins from biological fluids by use of an ionic liquid/aqueous two-phase system. *Chem.*−*Eur. J.* **2007**, *13*, 2130–2137.

(19) Li, C. X.; Han, J.; Wang, Y.; Yan, Y. S.; Xu, X. H.; Pan, J. M. Extraction and mechanism investigation of trace roxithromycin in real water samples by use of ionic liquid-salt aqueous two-phase system. *Anal. Chim. Acta* **2009**, *653*, 178–183.

(20) Jiang, Y.; Xia, H.; Guo, C.; Mahmood, I.; Liu, H. Phenomena and mechanism for separation and recovery of penicillin in ionic liquids aqueous solution. *Ind. Eng. Chem. Res.* **2007**, *46*, 6303–6312.

(21) Soto, A.; Arce, A.; Khoshkbarchi, M. K. Partitioning of antibiotics in a two-liquid phase system formed by water and a room temperature ionic liquid. *Sep. Purif. Technol.* **2005**, *44*, 242–246.

(22) Verna, J.; Kula, M. R. Extraction of proteins from biological raw material using aqueous PEG/citrate phase systems. *Biotechnol. Appl. Biochem.* **1990**, *12*, 397–404.

(23) Merchuk, J. C.; Andrews, B. A.; Asenjo, J. A. Aqueous two-phase systems for protein separation: studies on phase inversion. *J. Chromatogr., B* **1998**, *711*, 285–293.

(24) Zafarani-Moattar, M. T.; Hamzehzadeh, S. Liquid-liquid equilibria of aqueous two-phase systems containing polyethylene glycol and sodium succinate or sodium formate. *CALPHAD: Comput. Coupling Phase Diagrams Thermochem.* **2005**, *29*, 1–6.

(25) Huddleston, J. G.; Willauer, H. D.; Rogers, R. D. Phase diagram data for several PEG + salt aqueous biphasic systems at 25 °C. *J. Chem. Eng. Data* **2003**, *48*, 1230–1236.

(26) Pei, Y.; Wang, J.; Liu, L.; Wu, K.; Zhao, Y. Liquid-liquid equilibria of aqueous biphasic systems containing selected imidazolium ionic liquids and salts. *J. Chem. Eng. Data* **2007**, *52*, 2026–2031.

(27) Wu, B.; Zhang, Y. M.; Wang, H. P. Aqueous biphasic systems of hydrophilic ionic liquids + sucrose for separation. *J. Chem. Eng. Data* **2008**, *53*, 983–985.

(28) Wu, B.; Zhang, Y.; Wang, H. Phase behavior for ternary systems composed of ionic liquid + saccharides + water. *J. Phys. Chem. B* **2008**, *112*, 6426–6429.

(29) Li, C. X.; Han, J.; Wang, Y.; Yan, Y. Y.; Pan, J. M.; Xu, X. H.; Zhang, Z. L. Phase behavior for the aqueous two-phase systems containing the ionic liquid 1-butyl-3-methylimidazolium tetrafluoroborate and kosmotropic salts. *J. Chem. Eng. Data* **2010**; doi: 10.1021/je900533h.

(30) Zafarani-Moattar, M. T.; Hamzehzadeh, S. Phase diagrams for the aqueous two-phase ternary system containing the ionic liquid 1-butyl-3- methylimidazolium bromide and tri-potassium citrate at $T =$ (278.15, 298.15, 318.15 K). *J. Chem. Eng. Data* **2009**, *54*, 833–841.

(31) Guan, Y.; Lilley, T. H.; Treffry, T. E. A new excluded volume theory and its application to the coexistence curves of aqueous polymer two-phase systems. *Macromolecules* **1993**, *26*, 3971–3979.

(32) Wang, Y.; Hu, S. P.; Yan, Y. Y.; Guan, W. S. Liquid-liquid equilibrium of potassium/sodium carbonate + 2-propanol/ethanol + water aqueous two-phase systems and correlation at 298.15 K. *CALPHAD: Comput. Coupling Phase Diagrams Thermochem.* **2009**, *33*, 726–731.

(33) Rogers, R. D.; Bond, A. H.; Bauer, C. B.; Zhang, J.; Griffin, S. T. Metal ion separations in polyethylene glycol-based aqueous biphasic systems: correlation of partitioning behavior with available thermodynamic hydration data. *J. Chromatogr., B* **1996**, *680*, 221–229.

(34) Marcus, Y. Thermodynamics of solvation of ions. *J. Chem. Soc., Faraday Trans.* **1991**, *87*, 2995–2999.

(35) Othmer, D. F.; Tobias, P. E. Liquid-liquid extraction data - toluene and acetaldehyde systems. *Ind. Eng. Chem.* **1942**, *34*, 690–692.

(36) Zafarani-Moattar, M. T.; Seifi-Aghjekohal, P. Liquid-liquid equilibria of aqueous two-phase systems containing polyvinylpyrrolidone and tripotassium phosphate or dipotassium hydrogen phosphate: experiment and correlation. *CALPHAD: Comput. Coupling Phase Diagrams Thermochem.* **2007**, *31*, 553–559.

Received for review March 23, 2010. Accepted June 25, 2010. This work has been supported by the National Natural Science Foundation of China (No. 20777029, No. 20876071, and No. 20976074) and the Ph.D. Programs Foundation of Ministry of Education of China (No. 200807100004).

JE1002797